Assessment of windstorm-damage relations in the complex terrain of Norway

Ashbin Jaison[1,2], Asgeir Sorteberg[1,2], Clio Michel[1,2,3], and Øyvind Breivik[1,2,3]

[1]Geophysical Institute, University of Bergen, Bergen, Norway
[2]Bjerknes Centre for Climate Research, Bergen, Norway
[3]Norwegian Meteorological Institute, Bergen, Norway

Correspondence: Ashbin Jaison (ashbin.jaison@uib.no)

Abstract. Extreme winds are by far the largest contributor to Norway's insurance claims related to natural hazards. The predictive skills of four different damage functions are assessed for Norway at the municipality and national levels on daily and annual temporal scales using municipality level insurance data and the high-resolution Norwegian hindcast (NORA3) wind speed data for the period 1985-2020. Special attention is given to extreme damaging events and occurrence probabilities

5 of wind speed induced damages. Because of the complex topography of Norway and the resulting high heterogeneity of the population density, the wind speed is weighted with population. The largest per-capita losses and severe damages occur most frequently in the western municipalities of Norway, more exposed to incoming storms from the North Atlantic, whilst there are seldom any large losses further inland. There is no single damage function that outperforms others. However, a good agreement between the observed and estimated losses at municipality and national levels for a combination of damage functions

10 suggests their usability in estimating severe damages associated with windstorms. Furthermore, the damage functions are able to successfully reconstruct the geographical pattern of losses caused by extreme windstorms with a high degree of correlation. From event occurrence probabilities, the present study devises a damage classifier that exhibits some skill at distinguishing between daily damaging and non-damaging events at the municipality level. While large loss events are well captured, the skewness and zero-inflation of the loss data greatly reduces the quality of both the damage functions and the classifier for

15 moderate and weak loss events.

1 Introduction

Wind-related damage claims account for 56% of Norway's insurance payouts related to natural hazards from 1980 to 2017 and are by far the largest component of loss claims related to natural hazards (DSB Norway, 2019). They can affect all sectors from forests to marine and housing infrastructures (Jensen et al., 2010; Gardiner et al., 2013). However, a detailed

20 investigation into the relationship between Norwegian windstorms and damage has so far not been conducted for Norway. The comparison of different proposed storm damage models has only been conducted in a few countries due to a lack of long and sufficiently homogeneous insurance claims data (Cole et al., 2010; Prahl et al., 2015). Determining the best storm-damage model is important in order to make accurate predictions of future damages, whether it be in a few days (short-term forecast) or in many years (climate change range). In this paper, we investigate the relations between windstorms and their associated

25 damage by analysing 36 years of daily insurance data on the municipality level and daily maximum wind speed data using a set of storm-damage functions. Furthermore, we develop a probabilistic damage classifier that distinguishes between damaging and non-damaging wind speeds to help improve early warning systems.

Establishing robust windstorm-damage relations may help predict storm damage risk in the weather forecasting context (Merz et al., 2020) and evaluate the change in risk on the longer term in conjunction with climate change. Moreover, under-
30 standing the monetary risk involved in extreme wind events is crucial from the insurer's perspective to fix reasonable premiums and estimate portfolio risk. Several methods in the literature assess the risk associated with extreme wind events across various sectors such as agriculture, transport, and energy at varying spatial resolutions (Gliksman et al., 2023). Storm-damage functions are one such method which describes the mathematical relation between the intensity of a natural hazard, here the wind speed, and the monetary loss incurred due to the event. There are mainly two types of storm-damage functions: 1) the storm-based
35 approach, which links historical losses to wind speed information and 2) the hazard-based approach, which in addition makes use of micro-scale information such as the vulnerability, exposure and value of the assets. However, as detailed information about the damage is often proprietary, the most common approach, also used in the present study, is the storm-based approach (Dorland et al., 1999; Klawa and Ulbrich, 2003; Prahl et al., 2012, 2015). These storm-damage functions can also be split into deterministic and probabilistic types (Prahl et al., 2012). The deterministic damage functions do not estimate the uncertainty in
40 the wind speed-loss relation, whereas the probabilistic damage functions assume a statistical distribution for the model error. To make the deterministic and probabilistic models comparable, estimates from deterministic models are treated as equivalent to the mean of the estimates from the probabilistic models.

Storm-damage functions must be regionally fitted because they are highly dependent on local features. The number and spatial extent of the damages caused by extreme wind strongly depend on the exposure level of assets (Cardona et al., 2012),
45 which is connected to demography and economy both changing over time due to a variety of reasons such as urbanisation, higher infrastructure standards, economic growth, etc. Moreover, building types, building codes, differing insurance policies, claims settlement practices can also influence the performance of storm-damage functions (Walker, 2011) especially if they are not locally fitted. Norway has a complex topography with mountains and valleys and a rugged coastline with many fjords with a major share of the population living along the coasts and in the valleys (Simensen et al., 2021). Therefore, the population
50 density is an important factor to take into account when establishing storm-damage functions (Donat et al., 2011a).

A number of studies have investigated storm damage and risk on residential structures and other insured losses, mainly for Europe and more particularly Germany, using various damage functions and local information. Dorland et al. (1999) suggested a deterministic damage function by which loss increases exponentially with wind speed such that a slight increase in storm intensity can cause a significant increase in economic damage in the Netherlands and northwestern Europe. Meanwhile,
55 analysing annual insurance loss due to windstorms in Germany, Klawa and Ulbrich (2003) advocated a cubic relationship between the deviation in wind speed from its 98th percentile and the loss. Heneka and Ruck (2008) and Heneka and Hofherr (2011) applied a probabilistic damage function for Germany, which incorporates extreme value theory in conjunction with a non-linear function. However, this probabilistic damage function requires both claim and loss ratios, which are not common shared data and which we lack for Norway. To estimate the daily and annual losses at the district levels in Germany, Prahl

et al. (2012) proposed a power law-based probabilistic damage function where loss is proportional to a power of wind speed. They found out that the exponents range between 8 and 12, thus highlighting the need to fit the functions locally. Welker et al. (2016) simulated the spatial pattern of losses associated with historical windstorms that happened in Switzerland using the asset amount and the vulnerability, the latter depending on the wind gust. The agreement between the simulated loss and the observed insurance loss was shown to be reasonable but also case-dependent. They pointed to the uncertainty in the input data, such as in the wind gust but also in the estimation of the assets and vulnerability. More recently, Koks et al. (2020) developed an open-source hazard-based model that uses publicly available hazard, exposure and vulnerability data and the loss estimates can be treated as a baseline for further research. Using three different methods, Held et al. (2013) found a steady increase in the values associated with a 10-yr return loss by the end of the 21st century considering only the German private houses. Schwierz et al. (2010) suggested that, with climate change and increased storm intensity, Norway can expect a 16% increase in annual losses associated with windstorms. However, a recent study by Severino et al. (2023) indicated a significant decrease in winter storm damage over Norway.

In the following section, we introduce the insurance loss data and NORA3 hindcast wind speed data along with the different storm damage functions. In section 3, the climatology of the extreme winds and damages is presented in addition to the modelling results. We summarise and discuss the results in section 4.

2 Data and methods

2.1 Insurance loss data

We use daily insurance loss data, composed of the daily accumulated number of claims and monetary loss, from the Norwegian Natural Perils Pool for each of the 356 municipalities constituting Norway. The data span 36 years, from 1985 to 2020. The loss data distinguish losses by natural event types, such as floods, landslides, storm surges and windstorms. The present study focuses on the damages associated with windstorms.

Natural peril insurance is a compulsory part of the fire insurance held by almost all households in Norway (Sandberg et al., 2020). By the Norwegian Natural Perils Pool act, all buildings and movable properties which are insured against fire damage are also insured against natural disasters. All insurance companies underwriting fire insurance in Norway are obliged to become members of the Norwegian Natural Perils Pool and archive their losses. The fraction of households having fire insurance has stayed relatively constant over the period of interest; thus, the effect of varying market penetrations is small. In many previous studies, loss ratio and claim ratio, which are dimensionless, are used to model storm damage relations (Huang et al., 2001; Held et al., 2013; Prahl et al., 2015; Welker et al., 2016). However, Norwegian insurance does not include the total insured value, which prevents us from using the loss and claim ratios in the present study.

For long time series of loss data, it is necessary to account for inflation. To adjust for the effect of inflation, the insurance loss is modified using the Norwegian official consumer price index (CPI) at a fixed year (SSB Norway, 2023a). The base year for CPI in Norway is 2015, which we also use here. As an example, the relative difference of loss after inflation adjustment is of +60% for the New Year Storm (1992) and +7% Dagmar (2011).

Changes in exposure is another key variable that determines the intensity of losses incurred. Many studies use population as a proxy for exposure (see e.g., Simpson et al., 2014). Statistics Norway publishes yearly population data at municipality level which goes back to 1951 (SSB Norway, 2023b). To address the change in exposure to a certain extent, we compute the loss per person for each municipality by dividing the insurance loss data with the yearly population. Other factors, which may influence exposure, such as changing building standards and wealth distribution, are not accounted for in the present study.

A few extreme events have caused the majority of the total damage associated with windstorms. The five largest events were responsible for 4.3 bn. Norwegian Kroner (NOK) of damages (2015 values), which represents 36% of the total insurance loss from 1985 to 2020. The top damaging events and their associated losses are given in Table S1. As expected from the more intense cyclones reaching Norway in winter than in summer (Hoskins and Hodges, 2019), most extreme events occur between November and April. The presence of such extreme events brings skewness in the loss distribution and the absence of losses on most days of the year makes loss data zero-inflated (excess number of zeroes in data). The distribution skewness and the zero inflation (Fig. S1) in loss data is challenging for conventional fitting methods, such as the least-squares or maximum likelihood. Figure S1 highlights a record high number of claims in years 1994, 2015, and in a lesser extent 2011. This can be attributed to the storm of 1994, the storm Dagmar in 2011 and the storms Nina and Ole in 2015 (Table S1).

2.2 The wind speed data from the NORA3 hindcast

The high-resolution hindcast NORA3 covers the period 1979-2021 (and is being extended). The spatial resolution of NORA3 is 3 km×3 km, and surface variables are archived at hourly resolution. The non-hydrostatic, convection-permitting model HARMONIE-AROME (Seity et al., 2011; Haakenstad et al., 2021; Haakenstad and Breivik, 2022) ingests surface observations through a simple surface analysis scheme and blends this with initial fields from ERA5 (Hersbach et al., 2020). Boundary conditions are also taken from ERA5. The data is publicly available on the website https://thredds.met.no/thredds/catalog/nora3/catalog.html (last access 01 October 2023). The domain covers the North Sea, the Norwegian Sea, the Barents Sea, Svalbard and is bounded by Finland to the east. The hindcast consists in a sequence of 9-h forecasts initialised at 00, 06, 12 and 18 UTC every day from 1985 to 2020, which were the 36 years available at the time of our analysis. Aggregating the 4-9 h lead times provides an hourly dataset from which we extract the daily maximum wind speed and gust. NORA3 only slightly underestimates the maximum observed wind speed (Haakenstad et al., 2021; Solbrekke et al., 2021) and its interquartile range for the 10 strongest windstorms that affected Norway between 2009 and 2018 (Haakenstad et al., 2021), outperforming both the earlier hydrostatic 10-km Norwegian Hindcast Archive (NORA10, Reistad et al., 2011) as well as the recent ERA5 reanalysis.

2.3 Municipality level wind speeds

As the insurance loss is at the municipality level, we must estimate a municipality-relevant wind speed to apply the storm-damage functions. A simple approach is to average the daily maximum wind speed over all grid points contained in a given municipality. However, to compensate for the complex topography and disparate demography of Norway, we calculate a population-weighted wind speed to remove extreme wind events occurring over mountains, lakes, and other population-sparse regions. We make use of the gridded population data at 1 km×1 km for Norway for the period 2001 to 2019 (https://www.ssb.no/natur-

og-miljo/geodata; Strand and Bloch (2009)). As it does not cover the whole period of the study, we compute the average of population in each grid cell over the available period (2001-2019). Then this averaged population is remapped on the same 3 km×3 km grid as the NORA3 data. To achieve this, we assign each population grid cell to the nearest NORA3 grid cell. If more than one non-zero population grid cell corresponds to a NORA3 cell, we assign the sum of the population grid cells

130   to the NORA3 grid cell. Finally, in order to have the wind speed at the municipality level, as is the insurance data, we take the population-weighted average of the daily maximum wind speed in each municipality. We repeat the process for the daily maximum wind gusts.

2.4   Storm-loss models

Storm-damage functions connect the intensity of a storm event to the monetary damage caused by the storm. With the available

135   historical data of insurance loss and wind speed, we apply the storm-based approach to fit several storm-damage functions. The storm-damage functions discussed here are macroscale statistical models calibrated at the municipality level. Our key objective is to compare and assess the quality of various proposed storm-damage functions applied to our data. We employ three damage functions: the deterministic exponential model (Dorland et al., 1999; Huang et al., 2001; Murnane and Elsner, 2012), the deterministic model of Klawa and Ulbrich (2003) and the probabilistic function by Prahl et al. (2012). In addition,

140   we suggest a modified version of the Prahl model to better simulate the very steep damage curves found in some Norwegian municipalities. All damage models are fitted to loss per person to ensure uniformity among the storm damage approaches and easier inter-comparison of models and parameters. Finally, we devise a simple ensemble mean of the estimates from the four damage functions listed above, to check if it performs better than any of the four individual functions. In the following, we describe in detail the damage functions applied. From now on, L refers to the insurance loss, ν to the weighted wind speeds

145   and d to the damage function.

To fit and assess the skill of the storm damage models, we split the data into a testing and a training set. We assign the years from 1985-1989 and 2010-2012 to the testing part. The rest of the data from 1990-2009 and 2013-2020 is the training data. A necessary condition for splitting the data is that training and testing data should have identical distributions. We split the data so that both testing and training data include extreme storm events, the storm Dagmar in the testing data, and the New Year

150   storm in training data.

For robust storm-damage relations, extreme care should be taken while calibrating the damage functions. To make sure that the small losses, which are more frequent, are not better fitted than the high losses which are much less frequent, we bin the loss data with respect to wind speeds to reduce the weight of low loss events. Note that we do not perform binning for the Klawa damage function as the model is only suitable for high loss events and inherently decreases the number of zero and low losses

155   with the use of a high wind speed threshold. More about binning in individual models is explained in the following sections.

As many previous studies before (Donat et al., 2011b; Prahl et al., 2012, 2015; Pardowitz et al., 2016), we choose to fit the storm-damage functions at the municipality level. Despite the issue with a larger number of zero or low losses, this method is more meaningful and has the potential to be more accurate than doing fits using a country-averaged population-weighted wind speed. For example, the number of loss days when the population weighted wind speed exceeds its 98th percentile is high
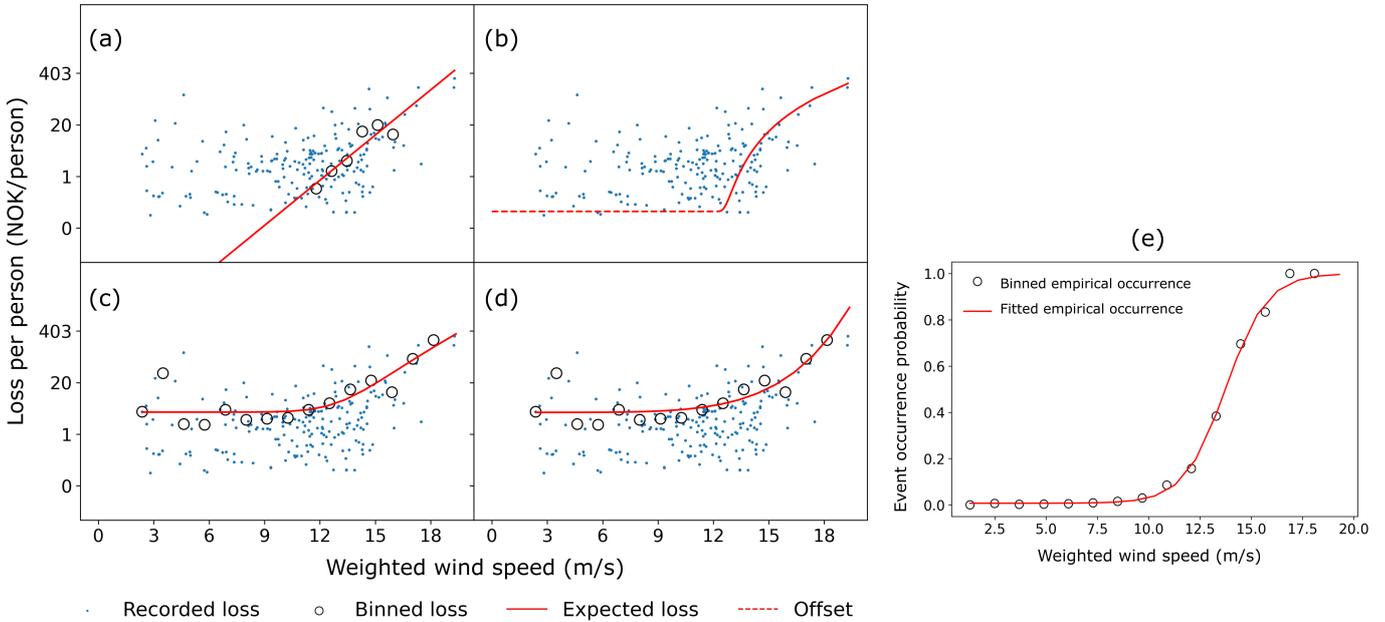
Figure 1. Shapes of the damage functions for an arbitrary municipality for (a) the exponential damage function, (b) the cubic excess over threshold damage function, (c) the magnitude term in the probabilistic damage function by Prahl, and (d) the magnitude term in the modified Prahl probabilistic damage function, (e) example of sigmoid function that estimates the probability of an event occurrence for an arbitrary municipality. The estimated parameters in this municipality are: γ_0=0.99, γ_1=0.99 and γ_2=13.75. Note that the y-axis for (a)-(d) is on a logarithmic scale and the zero loss on the y-axis is only for reference but the zero losses are not plotted/displayed.

along the Norwegian coast and low for further inland regions (Fig. S2a). Moreover, there are many local factors influencing the damage, such as building rules, building types, that promote local fits of the storm-damage functions. As a test, we pooled all municipalities together to perform the fits, but it didn't show any improvement in the estimation of both municipal and national level losses (Fig. S3).

2.4.1 Exponential model

The exponential damage function assumes that loss increases exponentially with increasing wind speed (Dorland et al., 1999). It is a simple damage function with only two parameters to be estimated and is formulated as,

$$d(\nu) = e^{\alpha(\nu - \beta)} \tag{1}$$

where α is the scale parameter and β is the location parameter. The loss is estimated from the damage function as $L(\nu) = d(\nu)$. The exponential model, by its shape, can be extended to lower wind speeds that may cause low to medium size losses. To take advantage of this, we choose the 95th percentile wind speed above which 82% of losses are recorded as the threshold for the exponential model. Such a threshold ensures that the model accounts for low to medium losses while discarding the

very small losses in the lower loss spectrum. The associated loss values are split into ten equally spaced bins with respect to the wind speeds and with a pre-condition that at least five loss days belong to each bin, as in Prahl et al. (2015). The binned losses are log-transformed, and with the assumption of normality, least square method are employed to estimate the model 175 parameters. Figure 1a shows the shape of the damage function with the red line.

2.4.2 Cubic-excess over threshold model

The damage function proposed by Klawa and Ulbrich (2003) suggests that the loss increases cubically for wind speeds beyond a certain threshold. The Klawa model was originally developed as a loss index for German districts and to estimate annual national losses using the German insurance data. Later, Pinto et al. (2012) calibrated the damage function for the affected areas 180 of individual storm events using the same insurance data. In the present study, we chose to calibrate the Klawa damage damage function with insurance loss at municipality level similar to Prahl et al. (2015) who applied it at district level on daily German insurance losses. This damage function is the third power of wind speeds above the 98th percentile scaled by the 98th percentile of the wind speed:

$$d(\nu) = \left(\frac{\nu - \nu_{98}}{\nu_{98}} \right)^3 \tag{2}$$

185 The loss is obtained by linear regressing the damage function:

$$L(\nu) = \beta_0 + \beta_1 d(\nu) \tag{3}$$

The intercept term β_0 in the fitted linear regression can be interpreted as the base loss, which is the loss estimate for all wind speeds below the 98th percentile. However, using this loss offset for all wind speeds below the 98th percentile doesn't allow to address the randomness in the lower loss spectrum. Figure 1b shows the model fit for this damage function (see the red solid 190 and dashed lines). β_1 is the slope of the line. The two β parameters are obtained using a least-squares regression method.

Several studies across Europe used the 98th percentile wind speed as a threshold for the Klawa damage function (Pinto et al., 2012; Karremann et al., 2014a, b). Ideally, the threshold for damaging wind should be locally chosen using statistically-determined estimates, but for simplicity we have kept the often used 98th percentile. In Norway, 72% of the insured losses are caused by wind speed above the 98th percentile. As the Klawa model is not designed for low loss cases, this is a fairly 195 reasonable simplification. Note that if grid point wind speeds are chosen, this choice of percentile can be problematic for places with weak winds, such as southeastern Norway (see Fig. S4a). To aleviate this, Karremann et al. (2014b) and Little et al. (2023) suggested a 9 m/s fixed threshold for wind speed causing damage in Norway. Our study uses the population-weighted averaged winds speeds, reducing the relative importance of grid cells with very low wind speeds and therefore avoiding the problem of very low 98th percentile. Note that even wind speeds above the 98th percentile can be associated with no loss. 200 Figure S2a shows that this often happens in southern inland regions of Norway, where it contributes to the uncertainty in the loss estimation.

2.4.3 Probabilistic damage function by Prahl

The power law based probabilistic damage function by Prahl et al. (2012) consists of a two-step fitting procedure: the first step estimating the occurrence probability of damage for a given wind speed and the second step estimating the loss magnitude. For both steps, we use wind speed bins and each bin must have at least five loss days, as (Prahl et al., 2015) did. We then fit the following sigmoid function to the binned wind speeds.

$$p(\nu) = 1 - \frac{\gamma_0}{1 + e^{\gamma_1(\nu - \gamma_2)}} \tag{4}$$

where the parameter γ_1 determines the steepness of the curve, γ_2 is the wind speed threshold beyond which the curve gets steeper and γ_0 determines the base probability of losses. Figure 1e shows the fit of the probability term (Eq. 4) of the damage function (see the red line). In addition, for a given wind speed ν, the magnitude of the loss M for non-zero losses is estimated through a power law-based function (Fig. 1c) and is related to the wind speed as follows:

$$M(\nu) = \sigma_0 + \left(\frac{\nu}{\sigma_2}\right)^{\sigma_1} \tag{5}$$

where σ_2 scales the wind speed, σ_1 is the shape parameter and σ_0 is the offset loss. The magnitude term is fitted on losses binned with respect to wind speeds.

The probability term makes use of the whole loss range while the magnitude term only uses non-zero losses. The probability of damage and the magnitude of loss are treated as independent variables. The damage function is then the product of the probability and the magnitude of loss:

$$d(\nu) = p(\nu)M(\nu) \tag{6}$$

The damage function includes the assumption that the observed losses follow a log-normal distribution ($M_{obs} \sim \mathrm{LN}(\mu, \sigma)$, where M_{obs} is the observed non-zero loss). Therefore, the expected loss for a given wind speed is

$$L = p(\nu)E(M(\nu)) \tag{7}$$

The probabilistic damage function by Prahl has a complex fitting procedure with eight parameters to be estimated. We refer the readers to the work by Prahl et al. (2015) to learn more about the parameters and fitting procedures of the model. The location (μ) and scale parameters (σ) of the log-normal distribution are estimated using the maximum likelihood method, and the other parameters of the damage function are estimated with the least squares method.

2.4.4 Modified probabilistic damage function by Prahl

The rationale behind Prahl's damage function is that the loss increases steeply for extreme wind events (Fig. 1c). However, based on inspection of the quality of the fitted curves for very high loss events, we identified a need for an even steeper damage function for certain municipalities in Norway. As the deterministic exponential damage function increases sharply and shows good fits for some of the municipalities, we propose a modified version of the damage function by Prahl that combines an

exponential fit with the probabilistic aspect of the Prahl model. The magnitude term in Eq. (5) of the Prahl damage function is modified as follows:

$$M(\nu) = \sigma_0' \exp\left[\left(\frac{\nu}{\sigma_2'}\right)^{\sigma_1'}\right] \tag{8}$$

The rest of the fitting procedure and assumptions are the same as for the Prahl damage function. The shape of the magnitude term in Eq. (8) is displayed in Fig. 1d with the red line.

2.4.5 Ensemble mean method

The four damage functions presented above have different advantages and drawbacks. The ensemble mean is calculated as the arithmetic mean of the loss estimates of the four functions, in the hope to improve the overall accuracy, as proven for ensembles of numerical weather/climate simulations.

2.5 Damage classifier

A damage classifier labels a given wind speed as damaging or not and adds useful information for event preparedness. The probabilistic damage occurrence probability function in Eq. (4) gives us the opportunity to define a classifier that distinguishes between a damaging and a non-damaging event. To build a robust classifier, it is necessary to define the probability threshold that separates an event from a non-event. With non-event days outnumbering the event days (class imbalance), it is not straightforward to define the probability threshold as 0.5 or to evaluate the model performance for various probability thresholds on the basis of traditional receiver operating characteristic (ROC) curves and the corresponding area under the curves (AUC). To circumvent the problem of class imbalance in identifying the best probability threshold, we employ the precision-recall curve and the associated F-scores (cf. section 2.6, Sokolova and Lapalme (2009)). Figure 2 shows the precision-recall curve for an arbitrary municipality. The split point of damage classifier corresponds to the probability threshold with the highest F-score from the precision-recall curve.

2.6 Model evaluation metrics

We evaluate the models' performance on the training and testing parts at the municipality level using the mean absolute error (MAE) and coefficient of variation (CV). In addition, the predictive skill of the probabilistic function in the Prahl damage function is evaluated using accuracy, recall, precision and F-scores.

As its name indicates, MAE is the mean of absolute differences between the observations and the model fits and is formulated as:

$$\text{MAE} = \frac{1}{n} \sum_{i=1}^{n} |y_i - \hat{y_i}| \tag{9}$$
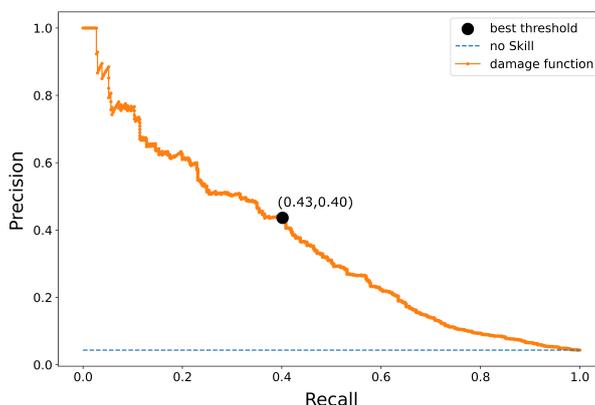
Figure 2. The precision-recall curve for an arbitrary municipality is shown with the orange line, the dashed blue line is the model with no skill, and the black dot corresponds to the point where the F-Score is maximum. In this example, the highest F-score of 0.41 is achieved at the probability threshold of 0.30. The precision and recall are shown in brackets.

where y_i is observed loss and $\hat{y}_i$ is the estimated loss. A high MAE indicates a poor skill of the model. Another evaluation metric used here is CV based on the root mean square error defined by Prahl et al. (2015) as follows,

$$\text{CV} = \frac{1}{\bar{y}} \left(\frac{1}{n} \sum_{i=1}^{n} (y_i - \hat{y}_i)^2 \right)^{\frac{1}{2}} \tag{10}$$

where $\bar{y}$ is the mean of the observed loss. High values of CV indicate large loss variability compared to the mean loss.

To quantify the classification skill of the damage classifier, we employ the precision, recall, accuracy and F-scores, which are defined as follows:

– Precision: The proportion of correctly classified positive samples to the total number of samples classified as positive.

– Recall: The proportion of correctly classified positive samples to the total number of positive samples.

– Accuracy: The proportion of correctly classified samples to the total number of samples.

– F-Score: Theoretically, the F-score is defined as the harmonic mean of precision and recall. It indicates the balance between precision and recall. F-score ranges between 0 and 1 and the higher the F-score the better. We take advantage of the F-scores to define the probability threshold for the damage classifier.

The binary damage classifier is optimized using the precision-recall curve and associated F-scores. The precision-recall curve is obtained by calculating the precision and recall for all potential probability thresholds obtained from the observed occurrence probabilities. The F-scores are computed for all points of the precision-recall curve (i.e. all probability thresholds) and evaluate the ability of each probability threshold to minimize false positives and capture true positives simultaneously. The probability threshold at which the F-score is maximum is chosen as the split point for the event classifier.

3 Results

In this section, we analyse the spatial and temporal spread of the insurance loss and compare the population weighted daily maximum wind speed, population weighted daily maximum wind gust and the daily maximum wind speed at the municipality level. We then compare the different damage functions along with the modified Prahl and ensemble mean models. However, considering the high degree of detail involved, we emphasize the following aspects, (1) daily losses at the municipality level, (2) top three extreme damaging wind events during the study period, (3) losses aggregated to the national level and (4) the probability function in Prahl et al. (2012) as a classifier. Furthermore, we discuss the pitfalls of the loss data, wind data and storm damage functions.

3.1 Overview of the windstorms losses

The municipalities on the west coast of Norway experience higher losses per person whereas there is hardly any loss further inland in southeastern Norway (Fig. S5a). Skewness and zero inflation are especially high for some municipalities in southeastern Norway where wind-related losses are rare. This data-scarcity greatly limits the performance of the damage functions.

The ten most damaging windstorms, in terms of cost, that reached Norway during the study period occurred between October and March and mainly affected central and southwestern Norway and more marginally Northern Norway (Table S1). An example of such a damaging storm is Dagmar in 2011 that affected western Norway causing more than one billion NOK of losses (Fig. S5b). The insurance losses caused by the ten largest events are given in Table S1 and represent a total of 5347 million NOK, which is 44% of the total losses due to windstorms between 1985 and 2020.

We find no significant temporal trends in the insurance losses caused by extreme winds. Trends in the losses time series, should arise from inflation or changes in wealth distribution. However, the effect of inflation is nullified by adjusting the insurance losses with the consumer price index and a change in wealth distribution is overlooked by the skewness in the losses. Therefore, the Mann-Kendall trend test we conducted on the annual national losses (Fig. S6) fails to detect any significant trend in losses.

The choice of wind data has the potential to influence the performance of the damage functions (Prahl et al., 2015). Also, the 98th percentile wind speed is widely regarded as critical from a damage perspective (Klawa and Ulbrich, 2003; Schwierz et al., 2010; Donat et al., 2011a). Figure S4a shows that the west coast and Northern Norway experience high magnitude wind events in comparison with southeastern municipalities. The 98th percentile of the population-weighted daily maximum wind speed exhibits a high correlation with the 98th percentile of the population-weighted daily wind gust (0.91) but a lower correlation with the 98th percentile of the unweighted daily maximum wind speed (0.61) (Fig. S4b). This difference can be attributed to the added information of population as weights for wind speed and emphasizes the importance of accounting for demography.

From the damage perspective, extreme damaging events are of the topmost concern. The losses above the 99.7th percentile (occurring on average around once a year) in each municipality when aggregated account for 85% of the total national loss. In each municipality, we define the losses higher than the 99.7th percentile as the extreme loss class and losses lying between the 98th and 99.7th percentiles as the high loss class. The high loss class comprises 8% of losses. The extreme loss class represents

approximately 31 and 9 extreme loss days in each municipality in the training and testing data, respectively. Segregation of losses into different classes helps to assess the performance of the damage functions for events of different severity.

310 By applying the different damage functions and calculating the ensemble means, we get daily fits of insurance loss for 10227 days in the training dataset and predictions for 2922 days in the test dataset for every municipality in Norway.

3.2 Municipality level loss estimations

To demonstrate the advantage of weighting wind speed with population, damage functions were also fitted with the original wind speed as the predictor variable. The prediction error on the test data shows that the population weighted wind speed has 315 lower CV in 67% of municipalities (see also Fig. S4c in supplement for the spatial distribution of where the original wind speed data performs better). From these results, we conclude that weighting wind speeds with population tends to improve the predictive performance of the damage functions. Therefore, from now on, we only use the population-weighted wind speeds when fitting the damage functions.

The deterministic damage models, that are the Klawa and exponential damage functions, perform best in nearly two thirds 320 of the municipalities across all losses classes in terms of MAE. Table 1 shows the performance of the four different damage functions defined in the methods section and of the ensemble mean for different loss classes. The deterministic models exhibit the smallest median MAE across all municipalities. Using the CV as the evaluation metric gives similar models performances as when using the MAE. The ensemble mean method does not massively outperform the competing models, but tends to give better results than the two Prahl's damage functions (Table 1). A map of the best model for each municipality exhibits a high 325 heterogeneity with no obvious spatial pattern, that is no model performing best in certain regions (Fig. S2b).

The spatial distribution of MAE is not uniform, but can be linked to the magnitude of the variance of losses, with municipalities with large loss variance having the largest MAEs (Fig. 3). In addition, the spatially heterogeneous distribution of losses (Fig. S5a) gives rise to spatially heterogeneous errors (Fig. 3b). The CV, which shows the extent of variability in losses in relation to the mean losses, exhibits a relatively heterogenous structure (Fig. 3c). On the one hand, there is tendency for high 330 CV in some inland municipalities of southeastern Norway, where the rarity of windstorms could be part of the reason. On the other hand, the northwest part of southern Norway also exhibits high CV although windstorms are more frequent there (Fig. 3b).

Pooling all municipality-level population-weighted wind speeds together to perform the storm-damage functions fits does not give better municipality-level losses estimations, as expected because of local effects, such as e.g. different population 335 density and vulnerability. The most skilled model in each municipality is associated with a larger MAE than when the fit is performed at municipality level (see Fig. S3a). This reduction of skill also occurs for the national-level losses (Fig. S3b).

3.3 Extreme damaging events

As extremely damaging windstorm events are of foremost importance, for example from the insurers' point of view, the ability of the damage functions to reproduce the damages associated with these events has to be assessed. To compare the estimated 340 and observed losses caused by major storm events, we sum the loss within the date range as given by the Norwegian Natural

Loss class	Damage function	Number of municipalities	MAE	CV
All loss days	Modified Prahl	32	31	245
	Prahl	46	28	238
	Klawa	134	22	212
	Exponential	91	24	218
	Ensemble mean	53	26	226
High loss class	Modified Prahl	16	5	184
	Prahl	25	5	176
	Klawa	141	4	156
	Exponential	99	4	134
	Ensemble mean	39	5	161
Extreme loss class	Modified Prahl	53	73	153
	Prahl	65	67	147
	Klawa	121	49	132
	Exponential	75	55	143
	Ensemble mean	42	66	143

Table 1. Number of municipalities for which a model performs the best, that is has the smallest MAE as a function of the loss class, as defined in the text. The medians of the MAE and CV on all 356 municipalities are also given. Note that the results are based on the performances on the unseen testing data. Also, some municipalities are not evaluated in the high loss class due to lack of data.

Perils Pool in Table S1. Using only the model exhibiting the best performance, on the whole testing period, in each municipality, we manage to reproduce the spatial pattern of the damages for the three most damaging wind storm events (Fig. 4, see Fig. S7 for estimates from individual models for the three most damaging wind storm events and Table S2 for their corresponding correlations. Also, Fig. S8 shows spatial patterns of seven other damaging events as given in Table S1.). Statistically significant

345 spatial correlations between the observed and estimated losses reaffirm the suitability of the damage functions to estimate the economic impacts of extreme damaging events.

In the extreme loss class, the probabilistic damage functions and the Klawa damage function perform best in a third of the municipalities each. The Klawa damage function also shows the smallest median error in the extreme loss class which is in agreement with previous comparison studies on storm damage functions over Germany (Prahl et al., 2015).

350 **3.4 National level loss**

Aggregating the municipality level loss observations and estimates yields a time series of daily national loss for each model and we find an overestimation of low-magnitude losses as all damage functions are calibrated in favour of extreme losses (Fig. 5). Moreover, the models' estimates capture well the magnitude and temporal evolution of the observed annual losses
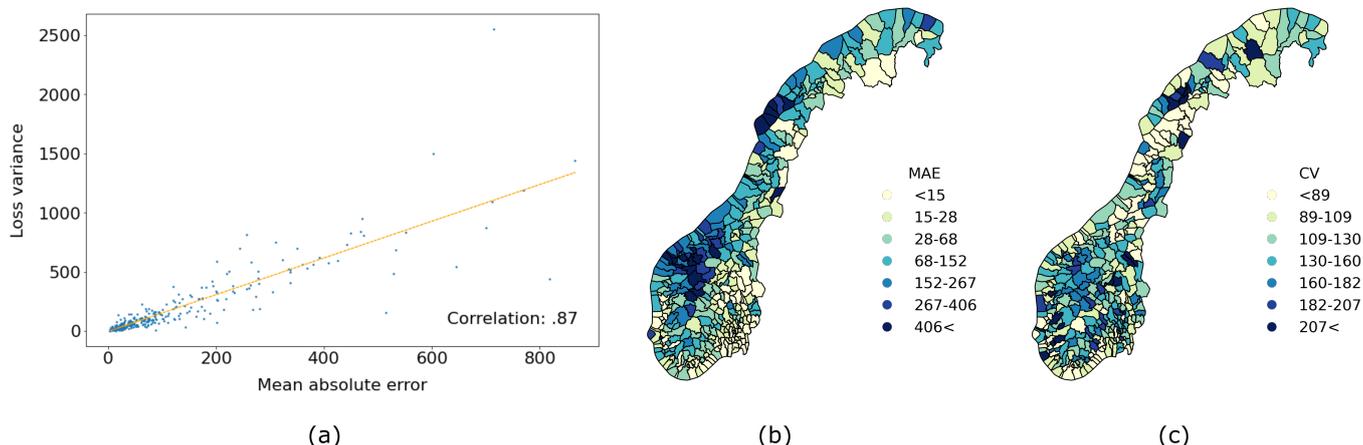
Figure 3. (a) Scatter plot of the loss variance against the smallest MAE for losses above the 99.7th percentile in the testing data where each dot represents a municipality. The orange line represents the linear trend obtained using a least squares regression with the correlation indicated in the bottom right corner. (b) Map of the smallest MAE among the five models in the extreme loss class fitted on the test data and (c) the corresponding coefficient of variation of the root mean square error. In (b) and (c), the legends have non-linear class boundaries at the 20th, 40th, 60th, 80th, 90th and 95th percentiles. Note that the results are based on the performances on the unseen testing data.

at the national level, with a Spearman rank correlation of 0.84 (Fig. 6). Figure 6 also reveals that the losses in the extreme

355 loss class are slightly overestimated in the training period in years where extreme storm events have occurred while there is an underestimation of loss in 2011 (part of testing data) when storm Dagmar occurred. The aggregated annual national level losses for individual models are shown in Fig. S9 and Fig. S10. Figure S9 shows that the deterministic models are well able to estimate losses in the extreme loss class at the national level. The probabilistic models overestimates the losses in certain municipalities by a large margin reducing the models' ability to estimate national level losses (Fig. S10). While fitting the

360 probabilistic damage functions, there are not enough extreme loss observations in certain municipalities, which prevents us from requiring a minimum number of loss observations in each bin. This one of the reasons for the very large differences between the observed and estimated losses for the probabilistic models.

3.5 Probability of damage occurrence

The damage classifier, devised here from the probability term in the Prahl's function (see section 2.6), demonstrates some skill

365 at predicting the most extreme events, but struggles for the weaker events. It correctly predicts the top five extreme events (Table S3) for over 70% of the municipalities. Even though we try to address the excess number of zeroes with the precision-recall curve, the classifier was only able to detect 20-40% of the actual damaging events in most municipalities (see the number of municipalities in the [0.2-0.4] interval in Fig. S11a) and zero events in around 15% of the municipalities ($\simeq$ 50 municipalities for the null true positive rate in Fig. S11a). Moreover, the false positive rate is small ($< 4\%$) in all municipalities (Fig. S11b).

370 Because of the noisy lower loss regime, the calculated probability thresholds are low (Fig. S12) for most municipalities with
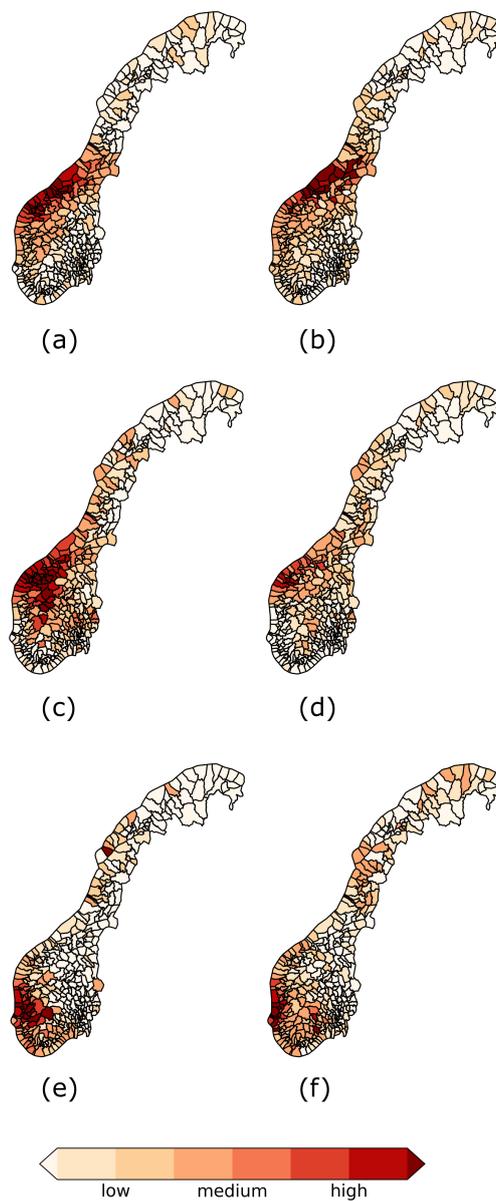
Figure 4. Spatial patterns of observed and estimated losses for the three most damaging events, where (a), (c) and (e) display the observed losses of the New Year storm, storm Dagmar and storm Nina, and (b), (d) and (f) are their respective estimates from the closest model to the observed loss in the testing period. The class boundaries of the colour bar are the 20th, 40th, 60th, 80th, 85th, 90th and 95th percentiles of the observed losses of their respective events. The spatial Spearman rank correlation between observed and estimated losses of the New Year storm, storm Dagmar and storm Nina are 0.67, 0.58 and 0.62 respectively. For each storm, we sum all the loss days as given in Table S1.
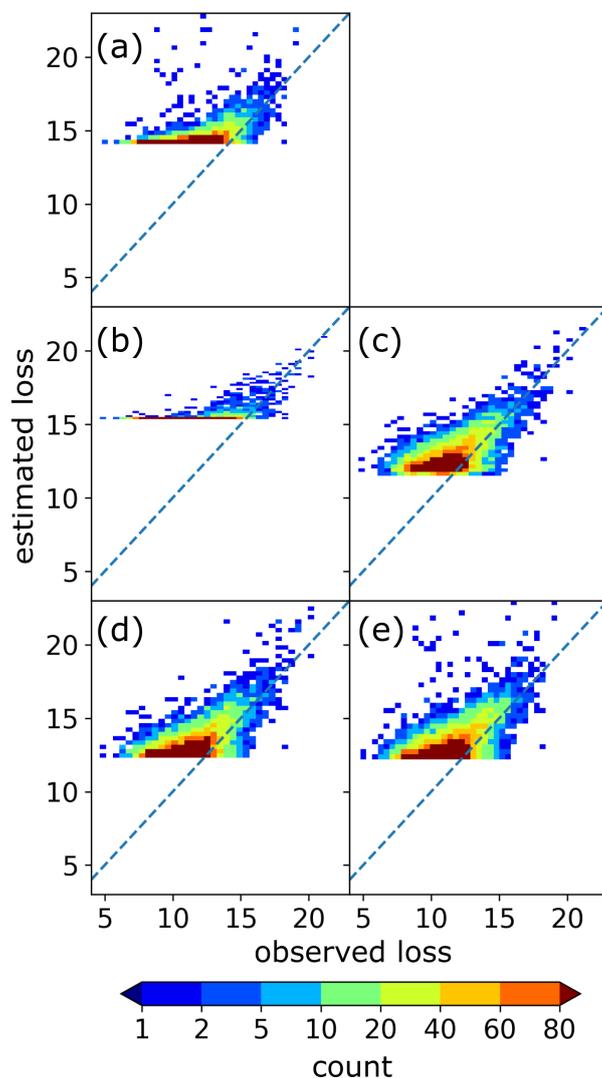
Figure 5. Observed and estimated daily losses (NOK) on log-log scale at the national level. Panels (a), (b), (c), (d) and (e) correspond to the ensemble mean method, the Klawa damage function, the exponential damage function, the Prahl damage function and the modified Prahl damage function, respectively. The dashed blue lines represent the 1:1 line.

values between 0.02 and 0.4 (median of 0.23, Fig. S12a). Only a few municipalities exhibit probability thresholds above 0.4, especially in southeastern Norway where damaging wind events are rare (Fig. S12b).

Although its skills are relatively poor, the damage classifier defined from event occurrence probabilities clearly outperforms a classifier that solely relies on wind speed. To demonstrate this, we define a damage classifier based on wind speed thresholds
375 in which all wind speeds above the 98th percentile are labelled as damaging (as is done in the Klawa model). A comparison
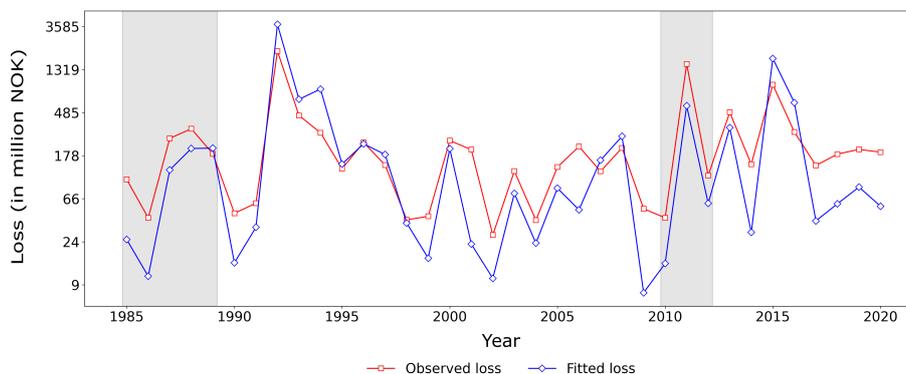
Figure 6. Annually-aggregated national losses using only the loss days in the extreme loss class from the insurance data (red line) along with the annual national loss estimates (blue line), which are the sum of each municipality's best-performing-model estimate (see also Table 1). Note that the y-axis is logarithmic and the shaded region represents the testing period.
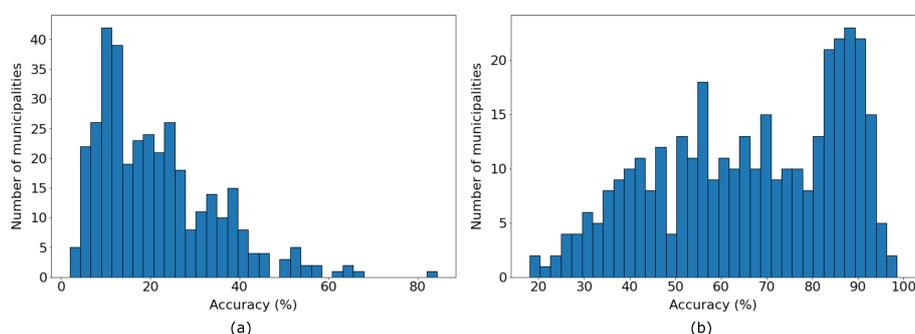
Figure 7. Distributions of (a) the accuracy of the damage classifier based on the wind speed 98th percentile (median: 18%) and of (b) the accuracy of the proposed damage classifier (section 2.5) devised from the Prahl damage function (median: 68%) for wind speeds above the 98th percentile, over all municipalities.

between these two classifiers shows far higher accuracy for the classifier using the probability threshold (Fig. 7b) than for the classifier using the wind speed classifier threshold (Fig. 7a).

4 Conclusions

Windstorms are the natural hazard that makes up more than half of the monetary losses in Norway. The capability of four
380 storm damage functions and their mean to reproduce the monetary losses associated with damaging wind events is evaluated for the complex topography and demography of Norway. The models' ability to reproduce spatial loss patterns of extreme loss events with a high degree of accuracy confirms the utility of both deterministic and probabilistic damage functions in estimating extreme loss events. However, the relatively poor performance of the damage/no-damage classifier points towards

the difficulty of developing an early warning system that encompasses also small loss events. Our results confirm the importance

385   of weighting wind speed with population, of locally fitting the storm-damage functions and of using various damage functions to best estimate the windstorms losses.

The deterministic Klawa model performs best in estimating extreme losses and this result is consistent with previous studies, such as Prahl et al. (2015). In our study, the Klawa model also exhibits the smallest error in the entire loss range. But, the Klawa model's inability to account for losses associated with wind speed below the 98th percentile greatly limits its applicability in

390   the lower loss range. The Prahl damage functions' have the ability to model the whole loss range and show the smallest error in a third of the municipalities. The models' performances suggest that relying on one single damage model may not be the best strategy if all the municipalities in Norway are to be modelled. The ensemble mean method mostly fails to outperform the individual models. Although the damage/no-damage classifier does very well at predicting extreme damaging events, more research is needed to propose a well-functioning damage classifier across all loss ranges.

395   There are several limitations to the damage functions including the inability of the models to account for the duration of the events and their tuning to model extreme losses at the expense of the low losses. Furthermore, the randomness of losses towards the lower loss spectrum diminishes the damage classifier's predictive skill. There are also certain pitfalls in the insurance data, such as incorrect reporting of time, location and type of claims. Also, the slight underestimation of maximum wind speeds in NORA3 may affect the shape of the damage curves. A direct comparison between other studies that employ damage functions

400   is not possible because the unit of loss in this study is NOK per person while most other studies use the loss ratio (insured loss/total value of the insured assets) instead of the actual insured loss.

Previous studies suggest that with climate change the intensity of future windstorms may increase (see, e.g., Priestley and Catto, 2022). It would be worthwhile to assess the future changes in windstorm-induced losses using the damage functions discussed here and future wind speed projections. Impact-based forecasting by which risks associated with a natural hazard are

405   predicted on the short term is gaining more popularity for climate risk management (Taylor et al., 2018; Zhang et al., 2019). The performance of these damage models, especially on regional level, suggests their utility for impact-based forecasting. However, to use trained storm-damage models on new data, one has to make sure that the distributions of the wind speed in the training dataset and the testing dataset are identical. To ensure this, statistical adjustments methods may be required. Also, from the risk modeling perspective, coupling the damage functions with the asset exposure, i.e. information on infrastructures

410   in addition to the population density, is a possible future direction.

Author contributions.   AJ: conceptualization, analysis, visualisation, interpretation of results, drafting of the paper. AS: conceived the idea, conceptualization, supervision of the work, funding, interpretation of results. CM: post-processing of NORA3 data. ØB: supervision of the work, funding. All authors contributed to drafting and reviewing the manuscript.

Competing interests.   The authors declare that they have no conflict of interest.

415 *Acknowledgements.* This work was funded by the Research Council of Norway through the project StormRisk nr 300608 granted to A. Sorteberg. We also thank the Norwegian Natural Perils Pool and the Norwegian Meteorological Institute for providing the data.

References

Cardona, O. D., Van Aalst, M. K., Birkmann, J., Fordham, M., Mc Gregor, G., Rosa, P., Pulwarty, R. S., Schipper, E. L. F., Sinh, B. T., Décamps, H., et al.: Determinants of risk: exposure and vulnerability, in: Managing the risks of extreme events and disasters to advance climate change adaptation: special report of the intergovernmental panel on climate change, pp. 65–108, Cambridge University Press, https://www.ipcc.ch/site/assets/uploads/2018/03/SREX-Chap2_FINAL-1.pdf, 2012.

Cole, C. R., Macpherson, D. A., and McCullough, K. A.: A comparison of hurricane loss models, Journal of Insurance Issues, 33, 31–53, http://www.jstor.org/stable/41946301, 2010.

Donat, M. G., Leckebusch, G. C., Wild, S., and Ulbrich, U.: Future changes in European winter storms losses and extreme wind speeds inferred from GCM and RCM multi-model simulations, Nat. Hazards Earth Syst. Sci., 11, 1351–1370, https://doi.org/10.5194/nhess-11-1351-2011, 2011a.

Donat, M. G., Pardowitz, T., Leckebusch, G., Ulbrich, U., and Burghoff, O.: High-resolution refinement of a storm loss model and estimation of return periods of loss-intensive storms over Germany, Natural Hazards and Earth System Sciences, 11, 2821–2833, https://doi.org/10.5194/nhess-11-2821-2011, 2011b.

Dorland, C., Tol, R. S., and Palutikof, J. P.: Vulnerability of the Netherlands and Northwest Europe to storm damage under climate change, Climatic change, 43, 513–535, https://doi.org/10.1023/A:1005492126814, 1999.

DSB Norway: Analyses of Crisis Scenarios 2019, https://www.dsb.no/globalassets/dokumenter/rapporter/p2001636_aks_2019_eng.pdf, 2019.

Gardiner, B., Schuck, A. R. T., Schelhaas, M.-J., Orazio, C., Blennow, K., and Nicoll, B.: Living with storm damage to forests, vol. 3, European Forest Institute Joensuu, https://efi.int/sites/default/files/files/publication-bank/2018/efi_wsctu3_2013.pdf, 2013.

Gliksman, D., Averbeck, P., Becker, N., Gardiner, B., Goldberg, V., Grieger, J., Handorf, D., Haustein, K., Karwat, A., Knutzen, F., Lentink, H. S., Lorenz, R., Niermann, D., Pinto, J. G., Queck, R., Ziemann, A., and Franzke, C. L. E.: Review article: A European perspective on wind and storm damage – from the meteorological background to index-based approaches to assess impacts, Natural Hazards and Earth System Sciences, 23, 2171–2201, https://doi.org/10.5194/nhess-23-2171-2023, 2023.

Haakenstad, H. and Breivik, Ø.: NORA3 Part II: Precipitation and temperature statistics in complex terrain modeled with a non-hydrostatic model, J Appl Meteor and Climatol, 61, 1549–1572, https://doi.org/10.1175/JAMC-D-22-0005.1, 2022.

Haakenstad, H., Breivik, Ø., Furevik, B. R., Reistad, M., Bohlinger, P., and Aarnes, O. J.: NORA3: A Nonhydrostatic high-resolution hindcast of the North Sea, the Norwegian Sea, and the Barents Sea, J. Appl. Meteor., 60, 1443–1464, https://doi.org/10.1175/JAMC-D-21-0029.1, 2021.

Held, H., Gerstengarbe, F.-W., Pardowitz, T., Pinto, J. G., Ulbrich, U., Born, K., Donat, M. G., Karremann, M. K., Leckebusch, G. C., Ludwig, P., et al.: Projections of global warming-induced impacts on winter storm losses in the German private household sector, Climatic Change, 121, 195–207, https://doi.org/10.1007/s10584-013-0872-7, 2013.

Heneka, P. and Hofherr, T.: Probabilistic winter storm risk assessment for residential buildings in Germany, Natural hazards, 56, 815–831, https://doi.org/10.1007/s11069-010-9593-7, 2011.

Heneka, P. and Ruck, B.: A damage model for the assessment of storm damage to buildings, Engineering Structures, 30, 3603–3609, https://doi.org/10.1016/j.engstruct.2008.06.005, 2008.

Hersbach, H., Bell, B., Berrisford, P., Hirahara, S., Horányi, A., noz Sabater, J. M., Nicolas, J., Peubey, C., Radu, R., Schepers, D., Simmons, A., Soci, C., Abdalla, S., Abellan, X., Balsamo, G., Bechtold, P., Biavati, G., Bidlot, J., Bonavita, M., Chiara, G. D., Dahlgren, P., Dee,

D., Diamantakis, M., Dragani, R., Flemming, J., Forbes, R., Fuentes, M., Geer, A., Haimberger, L., Healy, S., Hogan, R. J., Hólm, E., Janisková, M., Keeley, S., Laloyaux, P., Lopez, P., Lupu, C., Radnoti, G., de Rosnay, P., Rozum, I., Vamborg, F., Villaume, S., and Thépaut, J.-N.: TheERA5 global reanalysis, Quart. J. Roy. Meteor. Soc., 146, 1999–2049, https://doi.org/10.1002/qj.3803, 2020.

Hoskins, B. and Hodges, K.: The annual cycle of Northern Hemisphere storm tracks. Part I: Seasons, Journal of Climate, 32, 1743–1760, https://doi.org/10.1175/JCLI-D-17-0870.1, 2019.

Huang, Z., Rosowsky, D. V., and Sparks, P. R.: Long-term hurricane risk assessment and expected damage to residential structures, Reliability engineering & system safety, 74, 239–249, https://doi.org/10.1016/S0951-8320(01)00086-2, 2001.

Jensen, Ø., Dempster, T., Thorstad, E., Uglem, I., and Fredheim, A.: Escapes of fishes from Norwegian sea-cage aquaculture: causes, consequences and prevention, Aquaculture Environment Interactions, 1, 71–83, https://doi.org/10.3354/aei00008, 2010.

Karremann, M., Pinto, J., Von Bomhard, P., and Klawa, M.: On the clustering of winter storm loss events over Germany, Natural Hazards and Earth System Sciences, 14, 2041–2052, https://doi.org/10.5194/nhess-14-2041-2014, 2014a.

Karremann, M. K., Pinto, J. G., Reyers, M., and Klawa, M.: Return periods of losses associated with European windstorm series in a changing climate, Environmental Research Letters, 9, 124 016, https://doi.org/10.1088/1748-9326/9/12/124016, 2014b.

Klawa, M. and Ulbrich, U.: A model for the estimation of storm losses and the identification of severe winter storms in Germany, Nat. Hazards Earth Syst. Sci., 3, 725–732, https://doi.org/10.5194/nhess-3-725-2003, 2003.

Koks, E. et al.: A high-resolution wind damage model for Europe, Scientific reports, 10, 1–11, https://doi.org/10.1038/s41598-020-63580-w, 2020.

Little, A. S., Priestley, M. D., and Catto, J. L.: Future increased risk from extratropical windstorms in northern Europe, Nature Communications, 14, 4434, https://doi.org/10.1038/s41467-023-40102-6, 2023.

Merz, B., Kuhlicke, C., Kunz, M., Pittore, M., Babeyko, A., Bresch, D. N., Domeisen, D. I., Feser, F., Koszalka, I., Kreibich, H., et al.: Impact forecasting to support emergency management of natural hazards, Reviews of Geophysics, 58, e2020RG000 704, https://doi.org/10.1029/2020RG000704, 2020.

Murnane, R. J. and Elsner, J. B.: Maximum wind speeds and US hurricane losses, Geophysical Research Letters, 39, https://doi.org/10.1029/2012GL052740, 2012.

Pardowitz, T., Osinski, R., Kruschke, T., and Ulbrich, U.: An analysis of uncertainties and skill in forecasts of winter storm losses, Natural Hazards and Earth System Sciences, 16, 2391–2402, https://doi.org/10.5194/nhess-16-2391-2016, 2016.

Pinto, J. G., Karremann, M. K., Born, K., Della-Marta, P. M., and Klawa, M.: Loss potentials associated with European windstorms under future climate conditions, Climate Research, 54, 1–20, https://doi.org/10.3354/cr01111, 2012.

Prahl, B., Rybski, D., Kropp, J., Burghoff, O., and Held, H.: Applying stochastic small-scale damage functions to German winter storms, Geophys. Res. Lett., 39, https://doi.org/10.1029/2012GL050961, 2012.

Prahl, B. F., Rybski, D., Burghoff, O., and Kropp, J. P.: Comparison of storm damage functions and their performance, Nat. Hazards Earth Syst. Sci., 15, 769–788, https://doi.org/10.5194/nhess-15-769-2015, 2015.

Priestley, M. D. and Catto, J. L.: Future changes in the extratropical storm tracks and cyclone intensity, wind speed, and structure, Weather and Climate Dynamics, 3, 337–360, https://doi.org/10.5194/wcd-3-337-2022, 2022.

Reistad, M., Breivik, Ø., Haakenstad, H., Aarnes, O. J., Furevik, B. R., and Bidlot, J.-R.: A high-resolution hindcast of wind and waves for the North Sea, the Norwegian Sea, and the Barents Sea, Journal of Geophysical Research: Oceans, 116, https://doi.org/10.1029/2010JC006402, 2011.

Sandberg, E., Økland, A., and Tyholt, I. L.: Natural perils insurance and compensation arrangements in six countries, https://www.sintefbok. no/book/download/1259, 2020.

Schwierz, C., Köllner-Heck, P., Zenklusen Mutter, E., Bresch, D. N., Vidale, P.-L., Wild, M., and Schär, C.: Modelling European winter wind storm losses in current and future climate, Climatic change, 101, 485–514, https://doi.org/10.1007/s10584-009-9712-1, 2010.

495 Seity, Y., Brousseau, P., Malardel, S., Hello, G., Benard, P., Bouttier, F., Lac, C., and Masson, V.: The AROME-France Convective-Scale Operational Model, Mon Wea Rev, 139, 976–991, https://doi.org/10.1175/2010MWR3425.1, 2011.

Severino, L. G., Kropf, C. M., Afargan-Gerstman, H., Fairless, C., De Vries, A. J., Domeisen, D. I., and Bresch, D. N.: Projections and uncertainties of future winter windstorm damage in Europe, EGUsphere [preprint], https://doi.org/10.5194/egusphere-2023-205, 2023.

Simensen, T., Erikstad, L., and Halvorsen, R.: Diversity and distribution of landscape types in Norway, Norsk Geografisk Tidsskrift-
500 Norwegian Journal of Geography, 75, 79–100, https://doi.org/10.1080/00291951.2021.1892177, 2021.

Simpson, A., Murnane, R., Saito, K., Phillips, E., Reid, R., and Himmelfarb, A.: Understanding risk in an evolving world: emerging best practices in natural disaster risk assessment, Global Facility for Disaster Reduction and Recovery, The World Bank, UN International Strategy for Disaster Reduction, Washington, DC, https://www.gfdrr.org/sites/default/files/publication/Understanding_Risk-Web_Version-rev_1.8. 0.pdf, 2014.

505 Sokolova, M. and Lapalme, G.: A systematic analysis of performance measures for classification tasks, Information processing & management, 45, 427–437, https://doi.org/10.1016/j.ipm.2009.03.002, 2009.

Solbrekke, I. M., Sorteberg, A., and Haakenstad, H.: The 3 km Norwegian reanalysis (NORA3) – a validation of offshore wind resources in the North Sea and the Norwegian Sea, Wind Energy Science, 6, 1501–1519, https://doi.org/10.5194/wes-6-1501-2021, 2021.

SSB Norway: Consumer price index, https://www.ssb.no/en/priser-og-prisindekser/konsumpriser/statistikk/konsumprisindeksen, 2023a.

510 SSB Norway: Population 1 January and population changes during the calendar year (M) 1951 - 2023, https://www.ssb.no/en/statbank/table/ 06913/, 2023b.

Strand, G.-H. and Bloch, V. H.: Statistical grids for Norway, 9, https://www.ssb.no/a/english/publikasjoner/pdf/doc_200909_en/doc_200909_ en.pdf, 2009.

Taylor, A. L., Kox, T., and Johnston, D.: Communicating high impact weather: Improving warnings and decision making processes,
515 https://doi.org/10.1016/j.ijdrr.2018.04.002, 2018.

Walker, G. R.: Modelling the vulnerability of buildings to wind—a review, Canadian Journal of Civil Engineering, 38, 1031–1039, 2011.

Welker, C., Martius, O., Stucki, P., Bresch, D., Dierer, S., and Brönnimann, S.: Modelling economic losses of historic and present-day high-impact winter windstorms in Switzerland, Tellus A: Dynamic Meteorology and Oceanography, 68, 29 546, https://doi.org/10.3402/tellusa.v68.29546, 2016.

520 Zhang, Q., Li, L., Ebert, B., Golding, B., Johnston, D., Mills, B., Panchuk, S., Potter, S., Riemer, M., Sun, J., et al.: Increasing the value of weather-related warnings, Science Bulletin, 64, 647–649, https://doi.org/10.1016/j.scib.2019.04.003, 2019.